AIP | Applied Physics Letters

Nanostructured anatase-titanium dioxide based platform for application to microfluidics cholesterol biosensor

Md. Azahar Ali, Saurabh Srivastava, Pratima R. Solanki, Ved Varun Agrawal, Renu John, and Bansi D. Malhotra

Citation: Applied Physics Letters **101**, 084105 (2012); doi: 10.1063/1.4747714
View online: http://dx.doi.org/10.1063/1.4747714
View Table of Contents: http://scitation.aip.org/content/aip/journal/apl/101/8?ver=pdfcov
Published by the AIP Publishing

Nanostructured anatase-titanium dioxide based platform for application to microfluidics cholesterol biosensor

Md. Azahar Ali,[1,2] Saurabh Srivastava,[1] Pratima R. Solanki,[1] Ved Varun Agrawal,[1] Renu John,[2] and Bansi D. Malhotra[3,a)]
[1]*Department of Science and Technology Centre on Biomolecular Electronics, Biomedical Instrumentation Section, National Physical Laboratory, New Delhi-110012, India*
[2]*Department of Biomedical Engineering, Indian Institute of Technology Hyderabad, Andhra Pradesh-502205, India*
[3]*Department of Biotechnology, Delhi Technological University, Main Bawana Road, Delhi-110042, India*

(Received 16 May 2012; accepted 7 August 2012; published online 22 August 2012)

We report results of studies relating to the fabrication of a microfluidics cholesterol sensor based on nanocrystalline anatase-titanium dioxide (*ant*-TiO_2) film deposited onto indium tin oxide (ITO) glass. The results of response studies (optimized under the flow rate of 30 μl/min) conducted on cholesterol oxidase (ChOx) immobilized onto crystalline *ant*-TiO_2 nanoparticles (~27 nm)/ITO microfluidics electrode reveal linearity as 1.3 to 10.3 mM and improved sensitivity of 94.65 μA/mM/cm^2. The observed low value of K_m (0.14 mM) indicates high affinity of ChOx to cholesterol. No significant changes in current response of this microfluidics sensor are measured in the presence of different interferents. © *2012 American Institute of Physics*. [http://dx.doi.org/10.1063/1.4747714]

The integration of microfluidics with desired biomolecules has recently led to increased possibility to provide specific, sensitive, selective, accurate, and reliable miniaturized biosensing systems.[1–3] The miniaturized biosensor systems also referred to as micro total analysis systems or lab-on-a chip are known to have many advantages including small sample volumes leading to greater efficiency for detection of desired chemical reagents and low production cost. Besides this, the miniaturized systems allow easy disposability, high throughput synthesis, fast sampling times, accurate and precise control of samples and reagents eliminating the need for pipetting, and provide versatile format for integration of various detection schemes thereby leading to enhanced sensitivity.[4–9] These properties are considered to be very attractive for application as portable electrochemical microsystems. In this context, polydimethylsioxane (PDMS) is an interesting material for the development of the desired microsystems due to its high chemical resistance properties, low cost, optical transparency, and easy fabrication.[10]

Electrochemical detection is being increasingly used for enzymatic analysis, since it is an attractive choice for fabrication of microfluidics systems because of resulting higher sensitivity arising due to higher signal-to-noise ratio.[11] The size of the electrode is known to affect mass transport of the redox active species to and from the electrode surface and the bulk solution that may perhaps influence the electrochemical response. Incorporation of nanostructured metal oxides onto a microelectrode surface may help in increased loading of the desired biomolecules.[12] Among the various metal oxides, titanium dioxide (TiO_2) is a multifunctional material that offers many advantages like long-term stability, optical transparency, and good biocompatibility. Among the many polymorphs, anatase-TiO_2 (*ant*-TiO_2) is known to be high-purity single crystal with a high percentage of reactive (001) facets that may cause enhanced catalytic activity and selectivity.[13–16] This interesting material has been found to have many applications such as in photovoltaic cells,[17] photocatalysis,[18] photonic crystals,[19] gas sensors,[20] and biosensors.[21] The nano-TiO_2 may induce desired proteins to be adsorbed on the nano-sized surface and may perhaps provide effective orientation for electron transfer between a desired protein and the electrode.[22] The *ant*-TiO_2 nanobelts have been used for electrochemical determination of the perfect match and mismatch of single nucleobases at the physiological *p*H.[23] It has been reported that porous nanocrystalline TiO_2 film not only retains biological activity of enzymes, but it can also be used to load increased enzyme concentration.[24]

Cholesterol is known to play an important role in the brain synapses and in the immune system. The real time estimation of cholesterol is thus crucial for clinical diagnosis.[25–27] Many matrices including metal oxides and carbon nanotubes have been used to immobilize cholesterol oxidase (ChOx) for fabrication of cholesterol biosensor.[28–30] However, the integration of nanostructured metal oxide with a microfluidics device has not yet been explored. We report results of the studies relating to fabrication of a microfluidics cholesterol sensor based on ChOx functionalized with highly crystalline nanostructured *ant*-TiO_2. This nanostructured *ant*-TiO_2 based microfluidics device has not yet been utilized for fabrication a cholesterol sensor.

All chemicals including cholesterol and ChOx have been purchased from Sigma Aldrich. The ChOx (1 mg/ml) solution is freshly prepared in phosphate buffer (50 mM) at *p*H 7.0. The stock solution of cholesterol is prepared in 10% triton X-100 and is stored at 4 °C. The curing agent (Sylgard 184) has been obtained from Dow Corning (Midland, MI, USA). The SU8-100 negative photoresist and SU8 developer have been purchased from Microchem (Newton, MA, USA). Indium tin oxide (ITO) coated glass slides of thickness ~150–300 Å having a resistance of 50 Ω/sq have been procured from Vin Karola Instruments.

The characterization of the fabricated electrode has been carried out using x-ray diffractometry (XRD, Model Max 2200 diffractometer, Rigaku), atomic force microscope (tapping mode) [AFM, Model Multimode-V, Vicco Instrument], and Fourier-transform infrared spectroscopy (FT-IR, Model 2000,

a)Author to whom correspondence should be addressed. Electronic mail: bansi.malhotra@gmail.com. Telephone: 91-11-27871043 ext. 1609.

Perkin-Elmer). High resolution-transmission electron microscopy (HR-TEM, Model JEM-2000 EX, JEOL) and UV-visible spectroscopy (UV, Model 2200DPCV, Phoenix) studies have been used to characterize anatase TiO_2 nanoparticles. The electrochemical studies have been performed using an Electrochemical Analyzer (Model PGSTAT-30) in phosphate buffer saline (PBS; *p*H 7.0) containing 5 mM $[Fe(CN)_6]^{3-/4-}$ as a redox probe.

Two microelectrodes with dimensions 0.6 cm × 0.2 cm have been fabricated onto ITO coated glass slide by wet chemical etching process using ITO etchant [HNO_3:HCl:H_2O (1:10:10)] followed by washing with acetone and water. These electrodes are hydrolyzed using a solution containing H_2O:H_2O_2:NH_3 (5:1:1) for about 1 h at 70 °C. The slides are washed with de-ionized water and are dried in an oven at 100 °C for about 4 h.

Titanium (IV) butoxide is dissolved in 2-methoxy ethanol to prepare 5 (wt. %) precursor sol solution via drop wise addition of H_2O and nitric acid under continuously stirred condition to obtain hydroxide (Eq. (1)). The sol is then kept for aging for about 2 h at ambient temperature (25 °C) to polymerize the gel. The transparent sol-gel solution thus obtained is used to deposit film onto patterned ITO electrode on a glass substrate using dip coating method by selective masking the remaining part of glass slides with the help of a masking tape. The $Ti(OH)_4$ film is initially dried at ~110 °C for about 1 h and is finally annealed at 450 °C for about 2 h to form *ant*-TiO_2.

$$\begin{aligned} &Ti(OC_4H_9)_4 + HO-CH_2-CH_2-O-CH_3 \\ &+ H_2O \xrightarrow[\text{Sol}]{HNO_3,\text{Hydrolysis}} Ti(OC_4H_9)_2(OH)_2 \\ &+ 2C_4H_9OH \xrightarrow[\text{Gel}]{\text{Polycondensation}} [Ti(OH)_4].xHO-CH_2 \\ &-CH_2-O-CH_3.xH_2O \xrightarrow[\text{Amorphous gel}]{110\,^\circ C} Ti(OH)_4 \xrightarrow[\text{Titania}]{450\,^\circ C} TiO_2. \end{aligned} \quad (1)$$

10 μl of ChOx (1 mg/ml) was uniformly spread onto *ant*-TiO_2/ITO electrode and electrostatic interaction occurs between ChOx and *ant*-TiO_2 (Ref. 30) (Scheme 1). This ChOx/*ant*-TiO_2/ITO bioelectrode is rinsed with PBS to remove any unbound ChOx and stored at 4 °C when not in use.

The PDMS microchannels (200 μm × 200 μm × 2 cm) have been fabricated using standard procedures of soft lithography.[17] A master with the desired dimensions and pattern has been fabricated on a silicon wafer through ultra violet photolithography. The PDMS prepolymer and curing agent are mixed in a 10:1 ratio (v/v), degassed under vacuum, poured onto the master, and cured at 80 °C for 2 h. The PDMS replica is then carefully peeled off from the master. The reservoirs are fabricated by punching holes at desired positions in the PDMS slab. We have fabricated two channels that are essentially connected together to reservoirs with a single inlet and outlet. The principle reason to select two channels is to have increased sensor surface area. Again, the Reynolds number of the proposed microchannel is found to be very low as 0.166 indicating the fluid flow is completely laminar.

The PDMS assembly is clamped tightly to the glass substrate containing electrodes to ensure leakage free flow measurements. The electrochemical analyzer has been used for the electrochemical studies coupled directly to the three electrodes system of the microfluidics system. Ag/AgCl wire (dia: 0.6 mm) inserted directly into the outlet that acts as a reference electrode and a constant flow rate (30 μl/min.) of cholesterol solution is maintained with syringe pump (Harvard apparatus) during the experiments (Scheme 1).

XRD pattern from *ant*-TiO_2 powder [Fig. 1(a)] shows sharp peaks at 2θ: 25.4° and 48.2°, corresponding to the diffraction [101] and [200] planes indicating presence of the anatase phase of TiO_2. The diffraction pattern corresponding to [004], [105], [211], [204], [166], and [215] planes (JCPDS 89-4921, 89-6975) further supports the presence of anatase phase in TiO_2 with good crystalline structure. The size of anatase-TiO_2 nanoparticles obtained from the distinct peak (101) at 25.4° using Debye-Scherrer equation has been found to be as 15.4 nm and the crystallite strain of anatase-TiO_2 has been estimated to be as 2.9×10^{-3} using the Williamson and Hall plot.

Fig. 1(b) shows AFM images of nanostructured *ant*-TiO_2 on the ITO surface that are well-aligned, porous, mono-dispersed, and uniformly distributed. The average size of the *ant*-TiO_2 is found to be as ~27 nm [inset: Fig. 1(c), histogram plot]. The surface roughness of *ant*-TiO_2 electrode is ~0.63 nm. The *ant*-TiO_2 surface gets uniformly covered after it is functionalized with ChOx [Fig. 1(c)] and results in decreased roughness (0.49 nm) revealing that the nanosized *ant*-TiO_2 provides a favourable environment for adsorption of ChOx molecules via electrostatic interactions.

HR-TEM micrograph of the *ant*-TiO_2 (dispersed in methanol and deposited onto the copper grid by drop casting

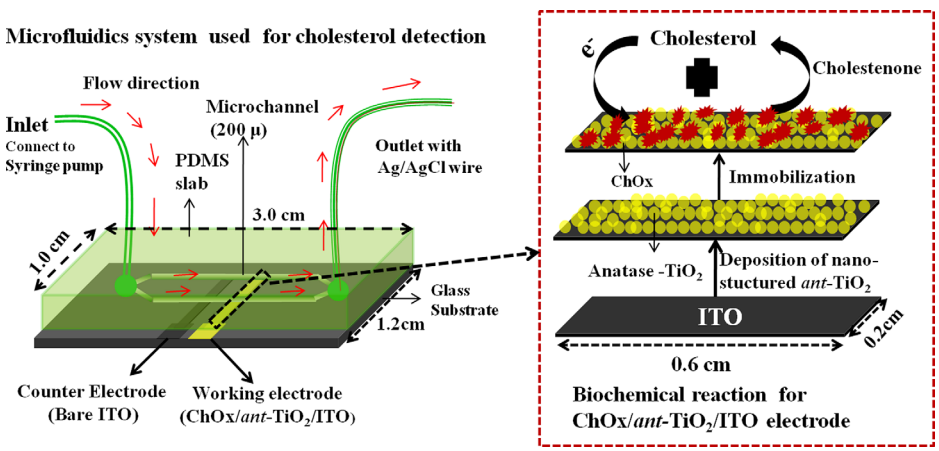

SCHEME 1. A microfluidics system for electrochemical detection of cholesterol.

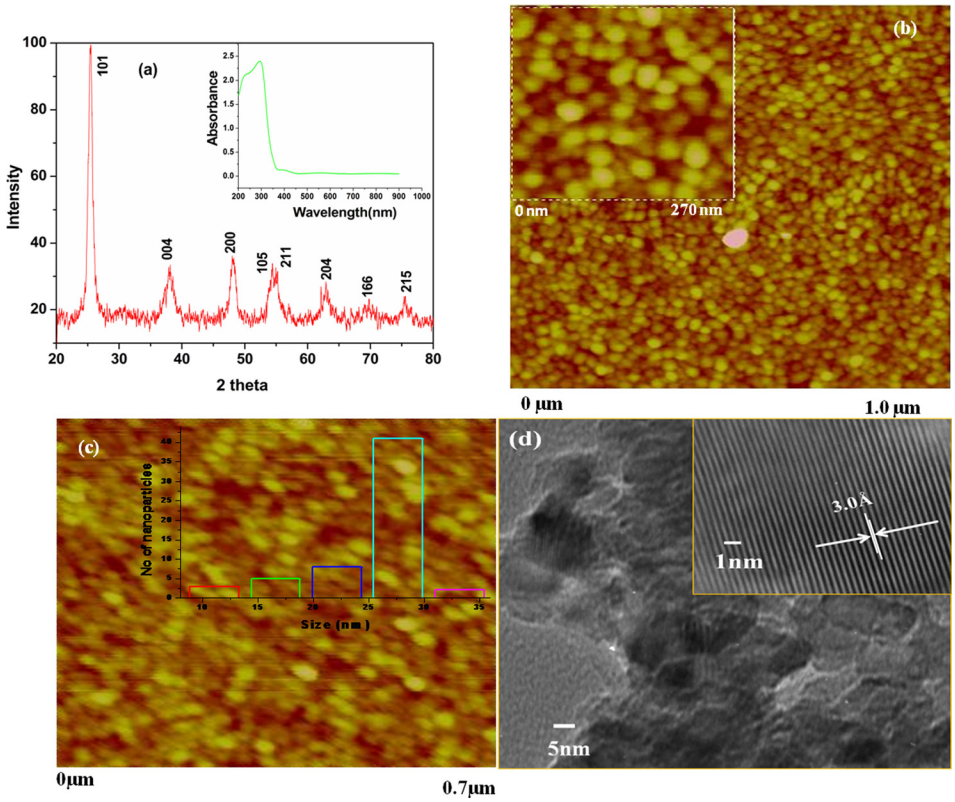

FIG. 1. (a) XRD spectrum of TiO_2 powder, inset: UV-visible spectra of *ant*-TiO_2/ITO film, (b) AFM for *ant*-TiO_2/ITO electrode, (c) AFM for ChOx/*ant*-TiO_2/ITO bioelectrode (inset: histogram plot for average size of *ant*-TiO_2 nanoparticles), and (d) HR-TEM studies of synthesis *ant*-TiO_2 nanoparticles (inset: lattice fringes of *ant*-TiO_2).

and dried in open atmosphere) clearly reveals cluster formed due to agglomeration [Fig. 1(d)]. The HR-TEM image [inset: Fig. 1(d)] shows the anatase polymorph of TiO_2 that is highly crystalline in nature. The presence of clear grain boundaries and lattice fringes is clearly seen in micrograph [inset: Fig. 1(d)]. The lattice separation of *ant*-TiO_2 is measured to be as ~3.0 Å, which matches with the d (101) spacing for the *ant*-TiO_2 tetragonal structure, which is in good agreement with results of the XRD studies.

The *ant*-TiO_2 has a broad absorption band from 280 to 400 nm in the UV region with a maximum absorption around 294 nm [inset: Fig. 1(a)]. A predominant blue shift in the absorption spectra due to quantum size effect of the nanocrystalline *ant*-TiO_2 compared to absorption spectra of the bulk TiO_2 is observed.[31] The optical band gap energy of these TiO_2 nanoparticles has been estimated to be as 3.4 eV, which is slightly higher than that of bulk anatase phase (3.2 eV).

The FT-IR spectra of *ant*-TiO_2/ITO exhibits characteristic peaks at 514 cm^{-1} corresponding to vibrational bending of Ti-O bonds in the finger print region [see Fig. S1 in supplementary material (SI)].[34] The peaks found at 844 and 1263 cm^{-1} correspond to C-H and C-O stretching bonds, respectively. The band seen at 3600 cm^{-1} is assigned to stretching and deformation of the O–H bond due to absorption of the water molecules. The FTIR spectra of ChOx/*ant*-TiO_2/ITO (Ref. 34) film (b) exhibits band at 1637 cm^{-1} arising due to N-H stretching in amide II indicating presence of ChOx on *ant*-TiO_2 film.

In the electrochemical impedance spectroscopy (EIS), electron transfer resistance (R_{CT}) that controls the electron transfer kinetics of the redox probe at the electrode interface is found to be as 23.0 kΩ (curve a) for *ant*-TiO_2/ITO electrode and decreases to 10.2 kΩ in the case of ChOx/*ant*-TiO_2/ITO bioelectrode (curve b) [see Fig. S2 in supplementary material (SI)].[34] These results reveal that a regular arrangement in the *ant*-TiO_2 nanocrystalline film with restricted orientation provides direct and faster electron communication between enzyme and the electrode surface.

The cyclic voltammetric (CV) studies have been conducted on *ant*-TiO_2/ITO (i) and ChOx/*ant*-TiO_2/ITO (ii) in the potential range of −0.5 V to +0.9 V at constant flow rate [Fig. 2(a)]. The anodic peak potential (E_{pa}) and cathodic peak potential (E_{pc}) for the ChOx/*ant*-TiO_2/ITO bioelectrode

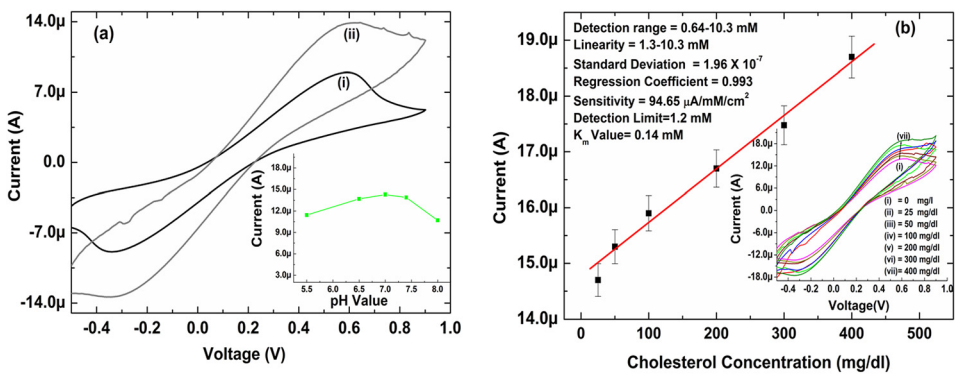

FIG. 2. (a) The CV of *ant*-TiO_2/ITO electrode (i) and ChOx/*ant*-TiO_2/ITO bioelectrode (ii) at scan rate (30 mV/s) in PBS (50 mM, *p*H 7.0, 0.9% NaCl) containing 5 mM $[Fe(CN)_6]^{3-/4-}$] [inset: *p*H studies of ChOx/*ant*-TiO_2/ITO bioelectrode] and (b) linear plot of response studies of ChOx/*ant*-TiO_2/ITO bioelectrode as a function of cholesterol concentration (0–10.3 mM) [inset: CV response of ChOx/*ant*-TiO_2/ITO bioelectrode with varying concentration of cholesterol].

have found to be as 0.598 V and −0.304 V, respectively. The magnitude of peak current (1.33×10^{-5}A) of ChOx/*ant*-TiO_2/ITO is found to be higher than that of the *ant*-TiO_2/ITO electrode (8.99×10^{-6}A). This is attributed to monodispersive nature of *ant*-TiO_2 that provides a suitable microenvironment for immobilization of ChOx. The observed excellent electrocatalytic characteristics of *ant*-TiO_2 reveal enhanced electron communication between active site of ChOx and the electrode.[32] These nanoparticles may directly communicate with active sites of the enzymes (ChOx and ChEt) and act as electron mediator that establish electronic path from active sites of the enzymes to the ITO electrode surface. Alternately, it may perhaps be assigned to the presence of strong electrostatic interactions and gibbosities on the *ant*-TiO_2 surface resulting in decreased tunneling distance between active site of ChOx and the electrode leading to enhanced peak current.[33]

The cyclic voltammetry studies of ChOx/*ant*-TiO_2/ITO bioelectrode have been conducted out as a function of scan rate from 30 to 100 mV/s at 30 μl/min [see Fig. S3 in supplementary material (SI)].[34] A proportional increase of redox current (I_a is anodic) with respect to square root of scan rate is observed indicating diffusion-controlled system [inset: Fig. S3 in supplementary material (SI)].[34] It is found that ΔE_p increases with the scan rate revealing facile electron transfer between the redox probe and electrode. The surface concentration (7.53×10^{-7} mol/cm^2) of ChOx/*ant*-TiO_2/ITO bioelectrode estimated from plot of I_p versus scan rate ($\nu^{1/2}$) using Brown–Anson model using Eq. (2).

$$I_p = \frac{n^2F^2I^*A\nu}{4RT} \tag{2}$$

where n is the number of electrons transferred, F is Faraday constant (96485.34 C mol^{-1}), A is surface area (0.004 cm^2), R is gas constant (8.314 J mol^{-1} K^{-1}), I^* is surface concentration of bioelectrode (mol/cm^2), T is 298 K, and I_p/ν is the slope of calibration plot. The diffusivity of ions $[Fe(CN)_6]^{4-/3-}$ for *ant*-TiO_2/ITO electrode has been calculated using Randle–Sevcik equation from CV response at various flow rates (1-50 μl/min) [see Fig. S4 in supplementary material (SI)].[34] It has been found that the diffusivity is maximum (3.38×10^{-4} cm^2/s) at an optimum flow rate of 30 μl/min. The plot between diffusivity and flow rate reveals that magnitude of diffusivity near the electrode surface increases with increased flow rate of solution [inset: Fig. S4 in supplementary material (SI)].[34] The higher diffusivity of the ions in the electrolyte is perhaps responsible for observed fast response time and higher sensitivity. This may be attributed to the higher diffusion rate of ions towards electrode as the diffusion distance decreases.

The effect of *p*H (5.0–8.0 at 25 °C) on ChOx/*ant*-TiO_2/ITO bioelectrode has been investigated using CV to estimate optimum enzyme activity [inset: Fig. 2(a)]. The highest current is obtained at *p*H 7.0 revealing that bioelectrode is most active at this *p*H. Thus, all the experiments are carried out at a *p*H of 7.0 at 25 °C.

Electrochemical response of the microfluidics sensor based on ChOx/*ant*-TiO_2/ITO bioelectrode as a function of cholesterol concentration (0.64–10.3 mM) is shown in Fig. 2(b). During electrochemical measurements, various concentrations of cholesterol are injected into the microchannels (0.8 μl/each channel) at a constant flow rate of 30 μl/min. The observed increased oxidation peak current may perhaps be due to fast charge transfer from flavin adenine dinucleotide (FAD) center of ChOx to the TiO_2 matrix (Scheme 1). The anodic peak current is found to increase linearly on addition of cholesterol and the linearity is obtained as 1.3–10.3 mM [inset: Fig. 2(b)]. The ChOx/*ant*-TiO_2 based-microsystem yields high sensitivity of 94.65 μA/mM/cm^2 as compared to that of the other cholesterol biosensors [see Table I in supplementary material (SI)].[34] The low value of Michaelis–Menten constant (K_m) obtained as 0.14 mM using Lineweaver–Burke plot reveals higher affinity between the active sites of ChOx onto the surface of *ant*-TiO_2 that perhaps directly participate in the biochemical reaction.

The selectivity of ChOx/*ant*-TiO_2/ITO bioelectrode has been determined by comparing magnitude of the current response by adding normal concentration of interferents such as glucose (5 mM), ascorbic acid (0.05 mM), uric acid (0.1 mM), urea (1 mM), and lactic acid (5 mM) to the cholesterol solution (2.6 mM) under same condition [see Fig. S5 in supplementary material (SI)].[34] The current response of this biosensing chip remains nearly same except for lactic acid/ascorbic acid wherein there is increase of about 5%. The bioelectrode achieves 95% of steady state current in less than 5 s indicating fast electron exchange between electrode and enzymes (data not shown). The reproducibility of different microfluidics bioelectrodes has been investigated using cholesterol concentration (2.6 mM) under identical conditions using CV response [see Fig. S6 in supplementary material (SI)][34] and it is found to be >3%. The storage stability of this bioelectrode has been determined by observing the current response using CV study at 2.6 mM cholesterol concentration at regular intervals of 7 days for about 35 days [see Fig. S7 in supplementary material (SI)][34] indicating that the bioelectrode exhibits a 97% response.

We have demonstrated the fabrication of a microfluidics sensor based on highly crystalline nanostructured *ant*-TiO_2 using PDMS microchannels for cholesterol estimation. This integrated microfluidics sensor provides improved sensitivity and low K_m value arising due to both higher surface-to-volume ratio of TiO_2 nanocrystals and small geometry of the microfluidics system. The reproducibility of different *ant*-TiO_2 bioelectrodes shows no significant changes of current response. This miniaturized microfluidics sensor requires minimal instrumentation and can be readily integrated with micro-electronics in a chip-based format. The electrochemical response of this microfluidics sensor depends upon flow rate of the solution that influences response time and diffusion coefficient. The efforts are being made to utilize this nanostructured *ant*-TiO_2 based electrode for estimation of other clinically important parameters like low density lipoproteins and total cholesterol.

We thank Director NPL, New Delhi, India for the facilities. We thank Mr. Sandeep Singh, NPL, New Delhi for the AFM studies. Md. Azahar Ali and Saurabh Srivastava are thankful to CSIR, India for the award of Research Fellowships. PRS is thankful to the DST for Fast Track Young Scientist award. VVA is thankful to CSIR for the Empowered project. We are thankful to Professor A. K. Mulchandani for the providing the microfluidic channels.

[1]D. C. Duffy, H. L. Gillis, J. Lin, J. Norman, F. Sheppard, and G. J. Kellogg, Anal. Chem. **71**, 4669 (1999).
[2]S. Kwakye, V. N. Goral, and A. J. Baeumner, Biosens. Bioelectron. **21**, 2217 (2006).
[3]A. Wisitsoraat, P. Sritongkham, C. Karuwan, D. Phokharatkul, T. Maturos, and A. Tuantranont, Biosens. Bioelectron. **26**, 1514 (2010).
[4]K. Morimoto and H. Suzuki, Biosens. Bioelectron. **22**, 86 (2006).
[5]V. N. Goral, N. V. Zaytseva, and A. J. Baeumner, Lab Chip **6**, 414 (2006).
[6]J. Wang, A. Ibanez, and M. P. Chatrathi, J. Am. Chem. Soc. **125**, 8444 (2003).
[7]M. A. Schwarz and P. C. Hauser, Lab Chip **1**, 1 (2001).
[8]L. Gervais, N. Rooij, and E. Delamarche, Adv. Mater. **23**, H151 (2011).
[9]S. Srivastava, P. R. Solanki, A. Kaushik, Md. A. Ali, A. Srivastava, and B. D. Malhotra, Nanoscale **3**, 2971 (2011).
[10]D. S. Zhao, B. Roy, M. T. McCormick, W. G. Kuhr, and S. A. Brazill, Lab Chip **3**, 93 (2003).
[11]H. Lee and S. Chen, Talanta **64**, 750 (2004).
[12]J. Min and A. J. Baeumner, Electroanalysis **16**, 9 (2004).
[13]J. F. Banfield and D. R. Veblen, Am. Mineral. **77**, 545 (1992).
[14]H. G. Yang, C. H. Sun, S. Z. Qiao, J. Zou, G. Liu, S. C. Smith, H. M. Cheng and G. Q. Lu, Nature **453**, 638 (2008).
[15]X. Q. Gong and A. Selloni, J. Phys. Chem. B **109**, 19560 (2005).
[16]S. Yurdakal, G. Palmisano, V. Loddo, V. Augugliaro, and L. Palmisano, J. Am. Chem. Soc. **130**, 1568 (2008).
[17]M. Gratzel, Prog. Photovoltaics **8**, 171 (2000).
[18]H. Choi, Y. J. Kim, R. S. Varma, and D. D. Dionysiou, Chem. Mater. **18**, 5377 (2006).
[19]B. Chen, F. Huang, Y. Cheng, and R. A. Carus, Adv. Mater. **21**, 2206 (2009).
[20]H. Tang, K. Prasad, R. Sanjinés, and F. Levy, Sens. Actuat. B **26–27**, 71 (1995).
[21]R. Doong and H. Shih, Biosen. Bioelectron. **22**, 185 (2006).
[22]Q. Li, G. Luo, J. Feng, Q. Zhou, L. Zhang, and Y. Zhu, Electroanalysis **13**, 413 (2001).
[23]J. Cui, D. Sun, S. Chen, W. Zhou, P. Hu, H. Liu, and Z. Huang, J. Mater. Chem. **21**, 10633 (2011).
[24]E. Topoglidis, A. E. G. Cass, G. Gilardi, S. Sadeghi, N. Beaumont, and J. R. Durrant, Anal. Chem. **70**, 5111 (1998).
[25]A. A. Ansari, A. Kaushik, P. R. Solanki, and B. D. Malhotra, Electron. Commun. **10**, 1246 (2008).
[26]R. Khan, A. Kaushik, P. R. Solanki, A. A. Ansari, M. K. Pandey, and B. D. Malhotra, Anal. Chem. Acta **616**, 207 (2008).
[27]P. R. Solanki, S. K. Arya, Y. Nishimura, M. Iwamoto, and B. D. Malhotra, Langmuir **23**, 7398 (2007).
[28]A. Kaushik, P. R. Solanki, K. Kaneto, C. G. Kim, S. Ahmad, and B. D. Malhotra, Electroanalysis **22**, 1045 (2010).
[29]A. A. Ansari, A. Kaushik, P. R. Solanki, and B. D. Malhotra, Appl. Phys. Lett. **92**, 263901 (2008).
[30]H. Cao, Y. Zhu, L. Tang, X. Yang, and C. Li, Electroanalysis **20**, 2223 (2008).
[31]G. Liu, C. Sun, H. G. Yang, S. C. Smith, L. Wang, G. Q. Lu, and H.-M. Cheng, Chem. Commun. **46**, 755 (2010).
[32]H.-L. Zhang, X.-Z. Zou, G.-S. Lai, D.-Y. Han, and F. Wang, Electroanalysis **19**, 1869 (2007).
[33]Q. Li, K. Cheng, W. Weng, P. Du, and G. Han, J. Mater. Chem. **22**, 9019 (2012).
[34]See supplementary material at http://dx.doi.org/10.1063/1.4747714 for results of FT-IR, EIS, diffusivity, scan rate, diffuisivity, selectivity, reproducibility, stability, and Table I.